A Molecular Model for the Strength of the Dielectric β Relaxation in Methyl Acrylate and Vinyl Acetate Polymers

Grant D. Smith and Richard H. Boyd*

Department of Materials Science and Engineering and Department of Chemical Engineering, University of Utah, Salt Lake City, Utah 84112

Received July 10, 1990; Revised Manuscript Received October 29, 1990

ABSTRACT: As a test of the supposition that flexible side-group motion is responsible for subglass relaxation in some polymers, a molecular model for the strength of the dielectric β subglass relaxation in poly(methyl acrylate) (PMA) and poly(vinyl acetate) (PVAc) homopolymers and their copolymers with ethylene (MA/E, VA/E) has been developed. The model is based on a rotational isomeric state (RIS) treatment for the overall relaxation, α glass–rubber relaxation + β process. The RIS model gives good agreement with the experimental total relaxation strengths for the homo- and copolymers in both systems. Then the RIS model is specialized for consideration of the β-process strengths only. A good account of the experimental behavior was obtained throughout the subglass temperature range for the β processes in both PMA and PVAc homopolymers, including the marked difference in strengths in the two systems and their strong temperature dependence. The strength of the β processes in the dilute copolymers is complicated by the possibility of additional contribution by main-chain subglass motions ("γ process") in the polyethylene segments. In MA/E copolymers the modeled process, which includes side-group motions only, accounts for about half of the measured strength. In VA/E experimentally the process is weak and has not been accurately quantified. The modeling results are consistent with the experimental behavior.

Introduction

The most prominent relaxation process in polymers is no doubt the glass–rubber (α) relaxation. It is due to long-range generalized segmental motion involving rotations about skeletal bonds. However, nearly all polymers show at least one additional relaxation process at temperatures that are well below the glass temperature where general segmental motion is frozen out.[1] The exact nature of the molecular motions associated with subglass relaxations remains obscure.[2] This is not due to the lack of suggestions for various types of motion but rather the lack of convincing models connecting the motions to the experimental measurements. One of the suggestions for molecular motions underlying subglass relaxations concerns polymers that have flexible side groups. It has been widely supposed that such groups may reorient largely independently of the main chain.[1] Dielectric relaxation is a good way to characterize such motions and our laboratory has been investigating experimentally some polymer systems where the side-group motions are presumed to be responsible for subglass (β) relaxation and should also be amenable to molecular modeling. In particular, dielectric data have been generated for polymers containing pendent ester groups as models for flexible side groups.[3,4]

There are two aspects to a molecular description of relaxation processes. First, there is the quasi-equilibrium behavior associated with complete relaxation that determines the strength of the process. Second, there are the dynamics that determine relaxation times and hence the time–temperature location. Strengths for subglass relaxations in general vary greatly from process to process in various polymers. They are very discriminating from the point of view of a model being able to successfully describe a process. Thus devising a successful model for strengths is a valuable step even though modeling of dynamics is also required for complete understanding. As commented on more fully below, it is reasonable to think that the strengths are dominated by *intra*molecular factors and an isolated chain model for the strength will be adequate.

The present work describes a detailed isolated chain molecular model for the relaxation strength in some pendent ester group polymers. These are poly(methyl acrylate) (PMA), poly(vinyl acetate) (PVAc), and their copolymers with ethylene (MA/E, VA/E), Figure 1. The copolymers provide an environment where the flexible ester side groups are chemically dilute and independent of each other, whereas in the homopolymers they interact significantly. The model proceeds by setting up a rotational isomeric state (RIS) description of the equilibrium mean-square moment for the PMA and PVAc homopolymers and the MA/E and VA/E copolymers. The mean-square moment leads to an overall relaxation strength, for the combined $\alpha + \beta$ relaxation. This requires generating Monte Carlo populations of chains of varying tacticity and, in the copolymers, of comonomer sequencing. Then a strength is derived for the subglass process by calculating the mean-square moment for chains where only the side groups may reorient and also taking into account the important effect of the molecular backbone being orientationally fixed in space in the glass. The latter calculation requires generating chain populations not only of representative comonomer and tacticity content but also of populations representative of individual chain conformations assumed to be frozen in at the glass temperature.

Comparison with experiment is accomplished via reducing experimental relaxation strengths to dipolar correlation factors using the Kirkwood–Onsager equation.[1,5] The latter is effectively the same as the quantity deduced from the model, i.e., the *dipole moment ratio*, the mean-square moment per dipolar group normalized by an effective group dipole moment. The argument for the isolated chain treatment of the molecular model being adequate is based on the expectation that *inter*molecular correlation effects on the measured correlation factors are minor compared to the *intra*molecular correlation. Dipolar correlation is effected primarily intramolecularly through the influence of the conformational states of connecting bonds, including those of the polymer skeleton. The correlation usually dies away fairly quickly as the number of intervening skeletal bonds increases. The present series of polymers provides a test of these effects, since the dipolar correlation from this source is quite appreciable in the homopolymers and should be negligible

0024-9297/91/2224-2731$02.50/0

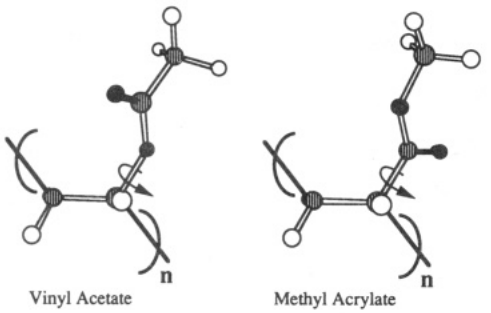

Figure 1. Ester group attachment in vinyl acetate (VA) and methyl acrylate (MA) environments.

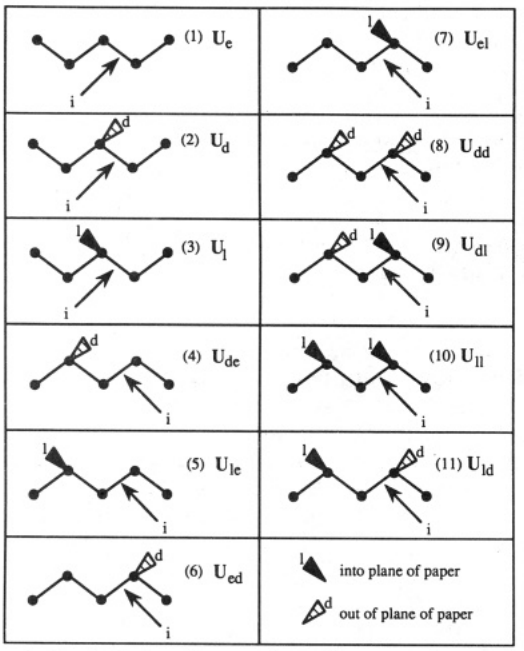

Figure 2. Statistical weight matrix environments in copolymers. Subscripts "*d*" and "*l*" refer to stereochemical sense in vinyl units; "*e*" refers to ethylene units.

in the chemically dilute copolymers.

The rotational isomeric state model is based on the interaction energy parameters developed in the previous paper.[6] These are used to set up appropriate statistical weight matrices. The side-group states are explicitly included along with main-chain states in the matrices. The RIS models differ from previous ones for PVAc[7] and PMA[8,9] homopolymers in this explicit, and in the present context essential, inclusion.

The Molecular Model

Statistical Weight Matrices. For vinyl–ethylene copolymers, considering only torsional interactions up to nearest neighbor, there are 11 possible bond environments or pairs of interdependent torsional states that need to be considered in the development of statistical weight matrices, as determined by the chemical and stereochemical structure of the monomer containing the bond of interest and the previous monomer. Following the notation of Mark,[10] these environments and their associated matrices are shown in Figure 2. Stereochemical *d,l* subscripts follow the convention of the preceding paper.[6]

Conformational energetics analysis[6] revealed that a five main-chain torsional state description was necessary. The relative energies of the three side-group minima are a function of the main-chain conformation. It was therefore determined that a 15-state model would be necessary to

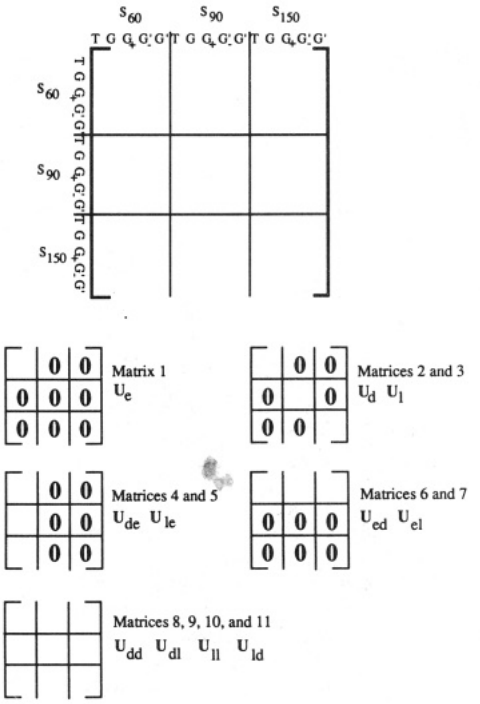

Figure 3. Structure of the statistical weight matrices. There are three side-group states for each of the five main-chain states. Numbers assigned to matrices refer to the environments of Figure 2.

model the copolymers, with five main-chain states for each of the three side-group states.

Figure 3 shows the general form of the 11 statistical weight matrices needed to describe the interdependent RIS model for the copolymer systems. Symmetry considerations indicate that there are only six unique statistical weight matrices, the others being determined by symmetry operations. The 15 × 15 matrices can be divided into nine 5 × 5 submatrices determined by the state of the side group associated with the previous and current bond. A side group is associated with the main-chain bond leading both up to it and away from it. Many of the submatrices are zero because many bonds are not associated with a side group (see Figure 2). The conformational energy parameters from Table II of ref 6 associated with each element of each matrix are determined by examination of the geometry of the local conformational environment as indicated by the matrix label and row and column indices. The completely enumerated matrices can be found elsewhere.[11]

Generation of Chemical and Stereochemical Structure. In modeling copolymer systems containing very long chains, a method must be devised to represent the chemical and stereochemical structure in terms of a finite set of chains of reasonable length such that computer calculations can be performed on a reasonable time scale. The method used in generating such chains is that described by Mark[10] for free radical polymerizing systems. The polymerization is assumed to be a first-order Markov process. The transition probability function **P** for the binary systems being considered is given by

$$\mathbf{P} = \begin{bmatrix} p_{11} & p_{12} \\ p_{21} & p_{22} \end{bmatrix} \tag{1}$$

The row index indicates the current radical type in a growing chain and the column index indicates the radical type after addition of a monomer unit. For example, p_{12} is the probability that a radical ending in monomer type

Table I
Composition of Generated Chains

chain	fraction polar actual	diad fractions,[a] actual (predicted)			
		M1M1	M1M2	M2M2	meso
MAx0.09	0.0867	0.0035 (0.0040)	0.1621 (0.1720)	0.8345 (0.8240)	b
PMA	1.0000	1.0000 (1.0000)	0.0000 (0.0000)	0.0000 (0.0000)	0.507
VAx0.05	0.0500	0.0031 (0.0025)	0.0900 (0.0925)	0.9069 (0.9025)	b
VAx0.20	0.1980	0.0450 (0.0400)	0.3200 (0.3200)	0.6350 (0.6400)	0.544
PVAC	1.0000	1.0000 (1.0000)	0.0000 (0.0000)	0.0000 (0.0000)	0.495

[a] M1 represents the vinyl monomer. Predicted long-chain values from Bovey et al.[16] [b] Number too small for statistical significance.

1 will add monomer type 2. The matrix elements are given by

$$p_{11} = \frac{r_1 f_1}{r_1 f_1 + f_2}, \quad p_{12} = \frac{f_2}{r_1 f_1 + f_2}, \quad p_{21} = \frac{f_1}{r_2 f_2 + f_1}, \quad p_{22} = \frac{r_2 f_2}{r_2 f_2 + f_1} \tag{2}$$

where r_1 and r_2 are reactivity ratios defined as

$$r_1 = k_{11}/k_{12}, \quad r_2 = k_{22}/k_{21} \tag{3}$$

where k_{ij} is the rate constant for the addition of monomer type j to a growing chain end of type i. The fractions of each monomer in the unreacted feed are given by f_1 and f_2. Assuming constant feed composition, the composition of the feed can be calculated from the composition of the long-chain polymer from the relationship

$$(F_1(r_1 + r_2 - 2) - r_1 + 1)f_1^2 + (2F_1(1 - r_2) - 1)f_1 + F_1 r_2 = 0 \tag{4}$$

where F_1 is the desired fraction of monomer 1 in the polymer.

Extensive tacticity and monomer distribution studies using proton and carbon-13 nuclear magnetic resonance techniques have been performed on PVAc and VA/E copolymers. These studies allow calculation of replication probabilities and reactivity ratios. For high-pressure VA/E free radical copolymerization, reported reactivity ratios[12-14] indicate that this system is ideally random, i.e., $r_1 = r_2 = 1$. VA/E copolymers were thus considered to be ideal for the purposes of chain generation. Tacticity studies[15] on the copolymer indicate random (atactic) Bernoullian behavior or a stereochemical replication probability $p_r = 0.5$. Studies on PVAc homopolymer[16-18] show Bernoullian behavior with p_r values ranging from 0.45 to 0.55, again almost completely atactic. A value of $p_r = 0.50$ was used in generating all VA/E copolymer and PVAc homopolymer chains.

PMA and MA/E copolymers have not been studied as extensively as their PVAc analogues. Matsuzaki et al.[19] performed carbon-13 NMR studies on a free radical polymerized PMA. The results indicated Bernoullian stereochemical behavior with a replication probability of 0.49. The MA/E copolymers studied experimentally in conjunction with this work were actually formed by esterification of poly(acrylic acid)/ethylene copolymers.[3] No monomer distribution studies were found for this system. Reactivity ratios can be estimated by using the empirical Q–e approach.[20] The reactivity ratios are given by the expressions

$$r_1 = \frac{Q_1}{Q_2}\exp[-e_1(e_1 - e_2)]$$

$$r_2 = \frac{Q_2}{Q_1}\exp[-e_2(e_2 - e_1)] \tag{5}$$

where the Q and e values are determined by fitting of the empirical equations above to a set of experimentally determined reactivity ratios for a large number of monomer pairs. The Q–e values for acrylic acid given by Ham[20] are 1.15 and 0.77, respectively, and for ethylene the values are 0.015 and −0.20. The reactivity ratios are therefore $r_1 = 36$ and $r_2 = 0.010$, where M_1 represents the vinyl monomer. Raetzsch and Lange[21] give the reactivity ratios for MA/E free radical copolymerization as $r_1 = 19.4$ and $r_2 = 0.023$. Since the comparisons with experiment have been made on quite chemically dilute copolymers, it makes almost no difference which set of values are used and the latter ones were employed in generating MA/E copolymer chains. A stereochemical replication probability of 0.5 was used for the PMA homopolymer and MA/E copolymers.

Once the transition probability matrix is known, the Monte Carlo techniques as described by Mark[10] can be applied. Entire sets of chains are rejected as not being representative if the occurrences of the monomers or diads in the generated chains lie outside allowable tolerances with respect to long-chain or predicted values, as discussed by Mark.[10] Monte Carlo[22,23] techniques, using the above replication probabilities, were also used to generate the stereochemical structure of the chains. Each chemical/stereochemical set consisted of 10 chains of 30 monomer units each. Table I shows the chemical and stereochemical composition of the generated chains for the compositions investigated.

It was found that end effects were not important in the calculation of the mean-square dipole moments or related properties for chains of 30 monomers or longer. The set label (e.g., MAx0.09) indicates the nominal mole fraction, x, of polar monomer. These compositions were chosen to approximately match experimental values studied. However, the notation has been altered from Buerger and Boyd.[2,3] There, MA20 designated the approximate *weight percent* MA and analysis found 9.2 mol %. Thus the statistical ensemble of chains represented by MAx0.09 corresponds to the experimental MA20. The VAx0.20 ensemble corresponds to the VA40 experimental sample.

Calculation of Mean-Square Moments. The mean-square value of any vector quantity associated with each bond of a chain molecule, averaged over the conformational space of the molecule, from the formalism of Flory[22] is given by

$$\langle m^2 \rangle = 2Z^{-1}\mathbf{h}^*\mathbf{G}_1\left[\prod_{i=2}^{n-1}\mathbf{G}_i\right]\mathbf{G}_n\mathbf{h} \tag{6}$$

where the generator matrix $\mathbf{G}$ has the form

$$\mathbf{G}_i = \begin{bmatrix} \mathbf{U} & (\mathbf{U}\otimes\mathbf{m}_{iT})||\mathbf{T}|| & \frac{\mathbf{m}_{i^2}}{2}\mathbf{U} \\ 0 & (\mathbf{U}\otimes\mathbf{E}_3)||\mathbf{T}|| & \mathbf{U}\otimes\mathbf{m}_i \\ 0 & 0 & \mathbf{U} \end{bmatrix}_i \tag{7}$$

The symbol ⊗ indicates the matrix direct product. The vectors $\mathbf{m}_i$ and $\mathbf{m}_i^T$ are the vector associated with the bond

i and its transpose. U is the statistical weight matrix and ||T|| the bond vector transformation supermatrix. In the terms $\mathbf{U}\otimes\mathbf{m}_i^T$ and $\mathbf{U}\otimes\mathbf{m}_i$ the moments are directly associated with each bond and matrix U to allow the dipole moment corresponding to each side-group state to be grouped with the corresponding states of the statistical weight matrix. The chain partition function, Z, is given by

$$Z = \mathbf{j}^*[\prod_{i=2}^{n-1}\mathbf{U}_i]\mathbf{j} \tag{8}$$

The average moment of a chemical/stereochemical set of chains, $\langle m^2\rangle_{C/S}$, is given as the result of calculating $\langle m^2\rangle_k$ for each chain, k, in the set and averaging over the number of chains, N_C, in the set, or

$$\langle m^2\rangle_{C/S} = (1/N_C)\sum_k \langle m_k^2\rangle \tag{9}$$

Generation of Chain Conformations. The fundamental assumption of the present model for subglass relaxation strength is that the main-chain conformations are frozen-in at the glass temperature but the side groups continue to reorient. Therefore the main-chain conformations at subglass temperatures are representative of conformational space at the glass transition temperature, while the conformations of the interacting side groups are functions of the ambient (subglass) temperature. A representative sample of main-chain conformations should therefore be generated at the glass transition temperature. Statistical mechanical averages are then performed on these fixed main-chain conformations, the side groups remaining flexible.

A Monte Carlo generation of conformations of a chain a step at a time employing a Markov process uses the conditional probability[24] $q_i(r,s)$ that the bond, i, being added is in state s, given the knowledge that the preceding bond is in state r. In terms of the a priori probability, $p_{i-1}(r)$, that bond $i-1$ is in state r and the a priori probability, $p_i(r,s)$, that bond i is in state s, while the preceding one is in state r

$$p_i(r,s) = p_{i-1}(r)q_i(r,s) \tag{10}$$

This relation serves to define $q_i(r,s)$ in terms of a priori probabilities.[24] The latter types of a priori probabilities may be found[25] as

$$p_i(s) = Z^{-1}\mathbf{j}^*[\prod_{j=2}^{j=i-1}\mathbf{U}_j]\mathbf{U}'_i(s)[\prod_{j=i+1}^{n-1}\mathbf{U}_j]\mathbf{j} \tag{11}$$

where $\mathbf{U}'_i(s)$ is the statistical weight matrix for bond i, with all elements except those for column s replaced by zeros, and $p_i(r,s)$ may be found by the same equation but with $\mathbf{U}'_i(s)$ replaced by $\mathbf{U}'_i(r,s)$, where the latter is the statistical weight matrix for bond i, with all elements except r,s set to zero. In practice in the present case to account for three side-group states, the states s, $s+5$, and $s+10$ and r, $r+5$, and $r+10$ under the numbering system used are exempted.

A Monte Carlo technique was used in conjunction with the conditional probabilities $q_i(r,s) = p_i(r,s)/p_{i-1}(r)$ to generate a set of main-chain conformations for each chain of each generated chemical/stereochemical set of chains discussed above. The generated conformations need to be a good representation of conformational space of the generated chains. Conformationally dependent properties such as the mean-square dipole moment averaged over the generated conformations should be similar to those values calculated by standard RIS matrix methods at the glass transition temperature. The mean-square moment for a generated fixed conformation at subglass temperatures is calculated from eqs 6–8 but with the statistical weight matrices $\mathbf{U}_i$ replaced by $\mathbf{U}_i(\phi_i)$ where now the latter is the statistical weight matrix appropriate for the bond i with all columns set to zero except the those associated with the main-chain conformational state ϕ_i. For each of the 10 chains of each chemical/stereochemical composition set of Table I, 100 conformations where generated. Table II shows a comparison of the mean-square dipole moment ratio averaged over the *generated conformations* with the value determined by matrix averaging over *all conformational space* for each chemical/stereochemical set of chains at the glass transition temperature. It may be seen that the generated conformations do a good job of representing the mean-square moments.

Table II
Comparison for Mean-Square Dipole Moment Ratios[a]

chain	mean-square dipole moment ratio (overall correlatn functn): from chain av	mean-square dipole moment ratio (overall correlatn functn): from generated conformatns
MAx0.09	0.99	1.01
PMA	0.65	0.64
VAx0.05	0.97	0.97
VAx0.20	0.89	0.91
PVAc	0.71	0.73

[a] Mean-sqaure dipole moment of a chain divided by the number of polar repeat units times the dipole moment of the polar repeat unit squared.

Overall Dielectric Relaxation Strength. The overall dielectric relaxation strength for a chain molecule describes the situation in which the polymers are able to visit all allowed conformations. For this case the relaxation strength can be formulated in terms of the Kirkwood–Onsager[1,5] equation (in SI form)

$$\epsilon_r - \epsilon_u = \left(\frac{\epsilon_u + 2}{3}\right)^2\left(\frac{3\epsilon_r}{2\epsilon_r + \epsilon_u}\right)\frac{1}{3kT\epsilon_0}(N_p g_p \mu_0^2) \tag{12}$$

where, ϵ_r and ϵ_u are the relaxed and unrelaxed dielectric constants, μ_0 is the vacuum value of a polar repeat unit dipole moment, k is Boltzmann's constant, T is the temperature, ϵ_0 is permittivity of free space, and N_p is the number of polar repeat units (dipoles) per unit volume. The quantity g_p is the correlation function of a polar repeat unit. If only the intramolecular correlation is considered, as discussed in the introduction, then g_p is given by

$$g_p = 1 + \frac{1}{n}\sum_{i=1}^{n}\sum_{j\neq i}^{n}\langle\cos\gamma_{ij}\rangle \tag{13}$$

where n is the number of dipoles per chain, γ_{ij} is the angle between the dipole moment vectors of the ith and jth dipoles of the chain, and the sums occur over all dipoles of the chain. Equivalently, g_p is given by

$$g_p = \langle m^2\rangle/n\mu_0^2 \tag{14}$$

where $\langle m^2\rangle$ is the mean-square dipole moment of the chain, the averaging occurring over all of conformational space of the chain as in eq 6. The experimental data and the statistical calculations are reduced to a convenient common basis through g_p. For the data, consisting of measurements of ϵ_r and ϵ_u, this is effected through eq 12 and for the calculations, resulting in mean-square moments, through eq 14.

If a system consists of a set of nonidentical chains of equal volume, an average correlation function value can

be calculated by averaging over all chains, k, or

$$\langle g_p \rangle = \frac{1}{N_C} \sum_{k=1}^{N_C} \frac{\langle m_k^2 \rangle}{\mu_0^2} \tag{15}$$

where N_C is the number of chains considered. For the case of a set of chains of varying chemical/stereochemical composition, comparison with eq 9 shows

$$\langle g_p \rangle = \langle m^2 \rangle_{C/S} / n\mu_0^2 \tag{16}$$

where n is the average number of dipoles per chain. With eq 16 the average correlation function or the relaxation strength for the overall process for any of the sets of generated chains in Table I can be calculated.

Subglass Dielectric Relaxation Strength. In the treatment of total relaxation strength above it is inherent in eq 13 or 14 that the averaging over conformational space also includes reorientation of the entire molecule over all spatial directions, not just internal reorientations. In the case of the subglass relaxation model the side groups relax relative to a fixed main chain and are not able to relax individually over all space. This has a strong effect on the relaxation strength and causes it to approach zero with decreasing temperature as individual dipoles become confined to their lowest energy state. The situation can be treated as follows. More generally, following Froehlich, $N_p g_p \mu_0^2$ in eq 12 associated with dipolar reorientation of N identical molecules per unit volume, where each individual, k, is capable of instantaneous configuration x and possessing moment $\mathbf{m}_k(x)$, is given by[26]

$$N_p g_p \mu_0^2 = N\langle \mathbf{m}_k(x) \cdot \mathbf{M}^* \rangle \tag{17}$$

where $\mathbf{M}$ is the moment of a spherical region large enough to be treated macroscopically that contains $\mathbf{m}_k(x)$ and $\mathbf{M}^*$ is the statistical mechanical average of $\mathbf{M}$, *with* $\mathbf{m}_k(x)$ *fixed*. $\langle \mathbf{m}_k(x) \cdot \mathbf{M}^* \rangle$ is the statistical mechanical average of $\mathbf{m}_k(x) \cdot \mathbf{M}^*$ over all configurations of $\mathbf{m}_k(x)$. The total moment $\mathbf{M}$ of the region is

$$\mathbf{M} = \sum_k \mathbf{m}_k \tag{18}$$

For the purposes of the present situation it is convenient to decompose the above into *inter*- and *intra*molecular terms as

$$\mathbf{M} = \mathbf{m}_k + \sum_{k'}{}' \mathbf{m}_{k'} \tag{19}$$

where k is a selected molecule with $\mathbf{m}_k(x)$ and the sum now runs over all other molecules, k'. Then

$$\langle \mathbf{m}_k(x) \cdot \mathbf{M}^* \rangle = \langle m_k(x)^2 \rangle + \sum_{k'}{}' \langle \mathbf{m}_k(x) \cdot \mathbf{m}^*_{k'} \rangle \tag{20}$$

where $\mathbf{m}^*_{k'}$ is the statistical mechanical average of $\mathbf{m}_{k'}$ with $\mathbf{m}_k(x)$ fixed. Under the assumed condition where *inter*molecular correlations vanish and only *intra*molecular correlations exist, $\mathbf{m}^*_{k'}$ will be independent of $\mathbf{m}_k(x)$ and therefore

$$\begin{aligned} \langle \mathbf{m}_k(x) \cdot \mathbf{M}^* \rangle &= \langle m_k(x)^2 \rangle + \sum_{k'}{}' \langle \mathbf{m}_k(x) \rangle \cdot \langle \mathbf{m}_{k'}(x) \rangle \\ &= \langle m_k(x)^2 \rangle + \langle \mathbf{m}_k(x) \rangle \cdot \sum_{k'}{}' \langle \mathbf{m}_{k'}(x) \rangle \end{aligned} \tag{21}$$

Above the glass temperature, each $\langle \mathbf{m}_{k'}(x) \rangle$ will spatially average to zero, leaving the conventional expression, eq 13 or 14, for the strength in terms of the mean-square moment of molecules with internal correlation but intermolecular uncorrelation. However, in the glass where overall molecular tumbling does not occur, $\langle \mathbf{m}_{k'}(x) \rangle$ need not average to zero. However, it is to be supposed that the *macroscopic* region associated with $\mathbf{M}$ is not permanently polarized and the average total moment of all molecules will be zero

$$\langle \mathbf{M} \rangle = \sum_k \langle \mathbf{m}_k \rangle = \langle \mathbf{m}_k(x) \rangle + \sum_{k'}{}' \langle m_{k'}(x) \rangle = 0 \tag{22}$$

or

$$\sum_{k'}{}' \langle \mathbf{m}_{k'}(x) \rangle = -\langle \mathbf{m}_k(x) \rangle \tag{23}$$

Therefore, from eqs 21 and 17, the per polar unit correlation function, g_p, of eq 12 is

$$N_p g_p \mu_0^2 = N\langle \mathbf{m}_k(x) \cdot \mathbf{M}^* \rangle = N[\langle m_k(x)^2 \rangle - \langle \mathbf{m}_k(x) \rangle \cdot \langle \mathbf{m}_k(x) \rangle] \tag{24}$$

Eq 24 with eq 12 forms the basis for computing the subglass relaxation strength. The mean-square moment, $\langle m_k(x)^2 \rangle$, above is for a fixed main-chain conformation and is to be evaluated as described earlier under Generation of Chain Conformations. The average moment of a chain, $\langle \mathbf{m}_k(x) \rangle$, is computed as follows. Let the molecular moment be written in terms of its constituent group dipole moments, μ_i, as $\mathbf{m}_k = \sum_i \mu_i$ and therefore

$$\langle \mathbf{m}_k \rangle = \sum_i \langle \mu_i \rangle \tag{25}$$

Let $p_i(s)$ be the a priori probability[25] that dipole i is in state s, i.e., averaged over the states of the other dipoles. Then

$$\langle \mu_i \rangle = \sum_s p_i(s) \mu_i(s) \tag{26}$$

The a priori probabilities, $p_i(s)$, are evaluated by matrix methods using eq 11, but with the $\mathbf{U}_i$ replaced by $\mathbf{U}_i(\phi_i)$, where again, as under Generation of Chain Conformations, the latter is the statistical weight matrix appropriate for the bond i with all columns set to zero except those associated with the main-chain conformational state ϕ_i. In practice, for comparison with experiment, g_p in eq 24 is to be taken as an average over the entire population of generated chains with frozen main-chain conformations and varying chemical and stereochemical sequencing.

A connection of the above treatment, as expressed in eq 24, with site models[27-29] for relaxation can be established by using $\mathbf{m}_k = \sum_i \mu_i$ and writing eq 24 as

$$N_p g_p \mu_0^2 = N[\sum_i \mu_i^2 - \sum_i \langle \mu_i \rangle^2 + \sum_i \sum_{j \neq i} \langle \mu_i \cdot \mu_j \rangle - \sum_i \sum_{j \neq i} \langle \mu_i \rangle \cdot \langle \mu_j \rangle] \tag{27}$$

and using

$$\langle \mu_i \rangle^2 = \sum_s p_i(s)^2 \mu_i^2 + \sum_s \sum_{r \neq s} p_i(r) p_i(s) \mu_i(r) \cdot \mu_i(s) \tag{28}$$

For the three states, $s = 1$, 2, and 3, considered in the present model and using $p_i(1) = 1 - p_i(2) - p_i(3)$ etc.

$$\langle \mu_i \rangle^2 = \mu_i^2[1 - 2p_i(1)p_i(2)(1 - \cos\alpha) - 2p_i(2)p_i(3)(1 - \cos\beta) - 2p_i(1)p_i(3)(1 - \cos\gamma)] \tag{29}$$

where α, β, and γ are the angles between the dipole vectors in states (1,2), (2,3), and (1,3), respectively. Thus, the per polar unit correlation function, g_p, is evaluated, identifying

Table III
Comparison of Calculated and Experimental Characteristic and Dipole Moment Ratios

		C_∞		D_∞	
homopolymer	temp, K	calcd	exptl	calcd	exptl
PMA	300	9.1	8.4 ± 0.5[a]	0.67[b]	0.67,[b] 0.67[c]
PVAc	303	9.3	9.4[d]	0.72[e]	0.70,[e] 0.89–0.94,[f] 0.75–0.80[g]
PVAc	339	8.6	8.4[d]		

[a] Uncertainty estimated by Yoon et al.[8] [b] Melt value from Figure 4, combined $\alpha + \beta$ processes. [c] Solution value quoted in ref 34. [d] Reference 32. [e] Melt value from Figure 6, combined $\alpha + \beta$ processes. [f] Solution value, ref 35. [g] Solution value, ref 36.

μ_i with μ_0, as

$$N_p g_p \mu_0^2 = N \sum_i \{\mu_0^2[2p_i(1)p_i(2)(1 - \cos\alpha) + 2p_i(2)p_i(3)(1 - \cos\beta) + 2p_i(1)p_i(3)(1 - \cos\gamma)] + \sum_{j\neq i}\langle\mu_i\cdot\mu_j\rangle - \sum_{j\neq i}\langle\mu_i\rangle\cdot\langle\mu_j\rangle\} \quad (30)$$

If, for example, there is but one dipole per chain, the dilute dipole limit, then eq 30 reduces to

$$N_p g_p \mu_0^2 = N\mu_0^2[2p(1)p(2)(1 - \cos\alpha) + 2p(2)p(3)(1 - \cos\beta) + 2p(1)p(3)(1 - \cos\gamma)] \quad (31)$$

This result is the same as a site model treatment of a three-state dipole.[27-29] Since the main-chain conformation is fixed, the p's are simple local Boltzmann factors expressing the site energies, U_s, and $p(s) = \exp(-U_s/kT)/\sum_s \exp(-U_s/kT)$.

Before invoking eq 24 or its equivalent, eq 30, in the circumstance of the present application, i.e., to ester side-group relaxation, it is necessary to note the following. The state labeled 1 is taken to be a "60°"-type side-group site and states labeled 2 and 3 to be the "90°" and "150°" sites of Figures 3 and 4 of ref 6. It is to be noted that although 2 and 3 appear to form distinct minima the *barrier* between the two sites is very small. This implies that dynamically, transitions between states 2 and 3 will be much more rapid than transitions between (1,2) and (1,3) and thus they will contribute in a relaxation region distinct from and at much lower temperature than the experimental β relaxations. That is, (2,3) transitions are assumed to be incorporated experimentally into ϵ_0 for the β process. Thus in evaluation of eq 30 the probabilities $p_i(1)$, $p_i(2)$, and $p_i(3)$ were all made on the basis of the three-state model but the correlation factor that gives rise to the strength is computed by leaving out the (2,3) terms. The angular excursion between states (2,3), i.e., the angle γ, is relatively small and at higher temperatures the effect of this omission is also relatively small. However, the site energy differences for (1,2) and (1,3) are considerably larger than for (2,3). Therefore at low temperature due to Boltzmann weighting there is a significant lowering of relaxation strength compared to including all of the transitions.

Results and Discussion

Characteristic Ratios. The characteristic ratio C_∞ is the limit as $n \to \infty$ of

$$C_n = \langle r^2\rangle_0/nl^2 \quad (32)$$

where $\langle r^2\rangle_0$ is the unperturbed mean-square end-to-end distance of the polymer chain, n the number of bonds, and l their length. Experimental values of C_∞ can be compared with values calculated via the RIS model as a valuable test of the conformational (RIS) model. Experimental values for the characteristic ratios of PMA[30,31] and PVAc[32] homopolymers are available. No experimental characteristic ratio data could be found for the MA/E and VA/E copolymers. For computational purposes, series of sets of atactic ($p_r = 0.5$) chains were generated. The series of chains ranged from 30 repeat units to 200 repeat units in length, each set of the series containing 40 chains except the set of 200 repeat unit chains, which consisted of 20 chains. Extrapolation of the C_n versus reciprocal molecular weight to infinite molecular weight yields C_∞ values. Table III compares the calculated C_∞ values with long chain experimental values. Agreement between calculated and experimental characteristic ratio values is seen to be good for both PMA and PVAc. This agreement supports the adequacy of the RIS models.

Experimental Dielectric Behavior. Before discussing the dielectric strength results from the modeling it is appropriate to review briefly the features of the experimental behavior[3,4] that a molecular model should account for. The α glass–rubber processes in both PMA and PVAc homopolymers show the effects of intramolecular correlation. The experimentally measured correlation factors are significantly less than unity. Both homopolymers show subglass β relaxation processes well separated from the α but there is a striking difference in the associated strengths in the two polymers. The subglass relaxation is considerably more prominent in PMA; its strength is a significant fraction of the overall relaxation strength, $\alpha + \beta$. It is much weaker and a relatively minor process compared to the process in PVAc. In MA/E copolymers, the prominence of the subglass β process, relative to the α, is maintained or enhanced compared to that in the homopolymer. The subglass process is shifted to lower temperature compared to that of the homopolymer, into a region comparable to the γ subglass process in PE. In VA/E copolymers, the behavior is more complex; the subglass process in isochronal temperature plots is split into two poorly resolved ones that have been labeled β and γ.[4] The subglass process strengths in all instances are relatively strongly temperature dependent, increasing with increasing temperature.

The role of subglass main-chain motions in the PE segments in the copolymers has been speculated upon.[4] It has been suggested that such motions occurring near vinyl units could cause rigid excursions of the ester groups that would contribute to the copolymer subglass strength in addition to that arising from the rotations of the ester groups about the attaching bonds. In MA/E copolymers where the subglass process occurs in the same temperature region as the PE γ process the two types of motion would be experimentally indistinguishable. In VA/E copolymers, it was suggested[4] that the β region arises from ester group rotations and the γ region from rigid side-group excursion driven by PE main-chain motions.

There is a feature of the experimental results for VA/E copolymers that needs comment. It was found that the correlation factors for the overall $\alpha + \beta$ processes in the more chemically dilute copolymers, where dipole–dipole correlation should be small, were not unity at all temperatures but approached unity at higher temperature.[4] This result was attributed to the fact that the measure-

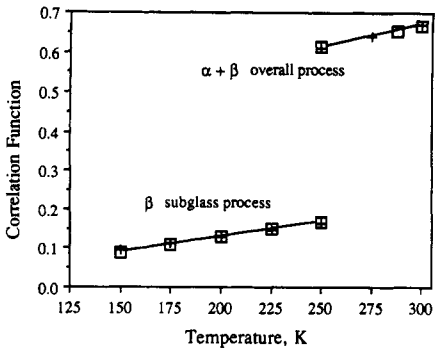

Figure 4. Comparison of calculated and experimental correlation functions for PMA homopolymer. Crosses are experimental; open squares are calculated.

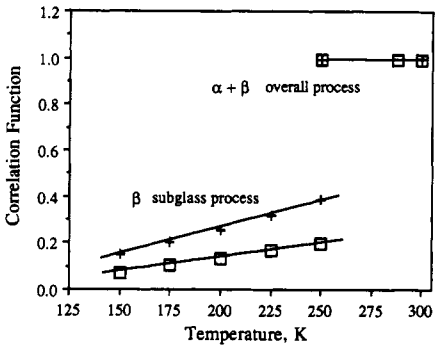

Figure 5. Comparison of calculated and experimental correlation functions for 9 mol % MA/E copolymer. Crosses are experimental; open squares are calculated.

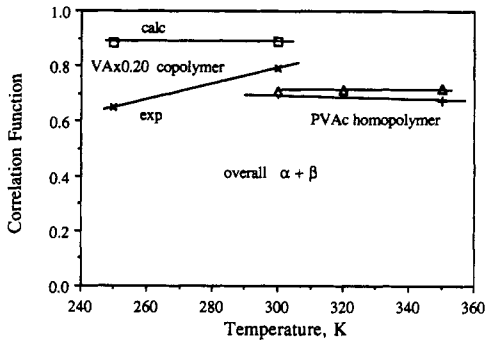

Figure 6. Comparison of calculated and experimental correlation functions for the α + β overall processes in PVAc and 20 mol % VA/E copolymer (VAx0.20). Open squares and triangles are calculated; + and × are experimental.

ments are actually made on specimens that are semicrystalline. It has been noticed that constraints on amorphous chain segments imposed by connections to the crystals can cause spatial restriction on complete dipole relaxation even in the glass–rubber relaxation region.[33] This results in an apparent correlation function for α + β processes that is less than unity at lower temperatures.

Comparison of Experimental and Calculated Relaxation Strengths. a. Overall Strength. The correlation functions for the combined α + β processes for PMA homopolymer and a chemically dilute MA/E copolymer (9 mol %) are shown in Figures 4 and 5, respectively. It is seen that the agreement between experiment and the calculations is excellent. For PVAc and a 20 mol % copolymer the results are shown in Figure 6. The agreement is good for the homopolymer. For the copolymer the calculated results are near but slightly less than unity as expected. Experimentally, the results only approach a value near unity with increasing temperature. This effect was mentioned above under the discussion of

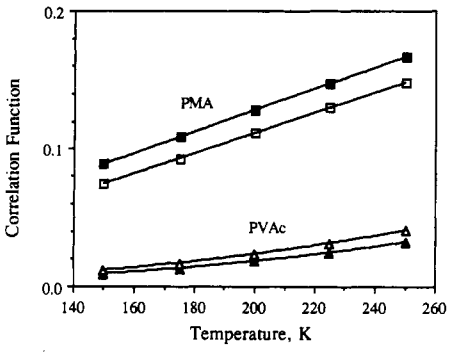

Figure 7. Effect of S_{60} (side-group position) statistical weight parameter adjustment on calculated subglass correlation functions. Squares are for PMA homopolymer; triangles are for PVAc homopolymer. Open symbols are for the original parameters of Table II, ref 6 (S_{60}(MA) = 0.97 kcal mol, S_{60}(VA) = 1.96 kcal/mol). Filled symbols are for adjusted values (S_{60}(MA) = 0.87 kcal mol, S_{60}(VA) = 2.22 kcal/mol).

the experimental behavior and ascribed to the experiments being made on a somewhat constrained amorphous phase in a semicrystalline environment.

The correlation factor g_p of eq 14 is seen to be the "dipole moment ratio" that is often determined from solution measurements. The experimental values in Figures 4 and 6 for the homopolymers were derived from melt measurements.[3,4] Comparison of the dipole moment ratios $D = g_p$ for the homopolymers with both solution[34-36] and melt measurements is made in Table III.

Results for overall relaxation strength displayed in Figures 4–6 are from calculations made with no adjustments to the energy parameters derived from the conformational energy calculations.[6]

b. Subglass Strength. In calculation of the subglass relaxation strengths it was apparent that they are especially sensitive to the statistical weight parameters S_{60}(MA) and S_{60}(VA) for the two systems. The site energy differences for side-group reorientation (see, for example, Figures 5 and 6 of the preceding paper) depend rather directly on this parameter. In turn, in the strength as expressed by eq 30, the Boltzmann weighted products, $p(1)p(2)$ and $p(1)p(3)$, are largely determined by this parameter. At the temperatures of the subglass regions, ~200 K, a few hundred calories has a strong influence on the strength. It is beyond the power of conformational energy calculations to predict energy differences at the level of 100 cal/mol. Figure 7 shows the effect on the correlation functions for the subglass processes of adjusting S_{60}(MA) from the value 0.97 kcal/mol in Table II ref 6 to 0.87 kcal/mol and S_{60}(VA) from 1.96 to 2.22 kcal/mol. This has a negligible effect on the calculated overall α + β strengths. Results for subglass β processes in PMA and MA/E calculated from these adjusted values are displayed along with the overall α + β correlation functions in Figures 4 and 5. The subglass strengths for the VA system are very small compared to the overall strengths in Figure 6 and are plotted separately on an expanded scale in Figure 8. With this minor parameter adjustment the calculated strengths of the subglass processes in the homopolymers are in good agreement with experiment. This includes the slopes with temperature as well as the absolute level of values. For the MA/E 9 mol % copolymer, it is to be seen in Figure 5 that the calculated values fall significantly below the experimental ones. We attribute this circumstance to the side-group reorientations accounting for only part of the strength, the rest coming from rigid side-group excursions driven by subglass main-chain motions in the PE segments. The latter are in a coincident temperature–frequency region with the side-group motions.

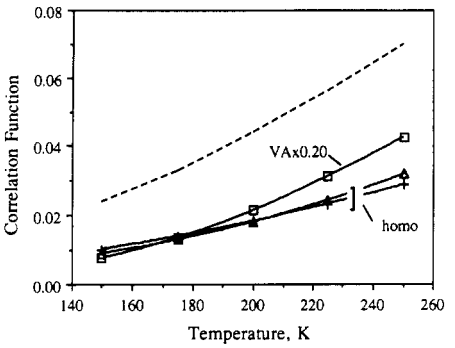

Figure 8. Comparison of calculated and experimental β subglass process correlation functions for PVAc homopolymer and 20 mol % VA/E copolymer (VAx0.20). Crosses are experimental; open symbols are calculated. There is no quantitative value for the experimental strength of the copolymer process. The dashed line is the experimental value for the lower temperature γ process in the copolymer and it is believed that the experimental β subglass process is somewhat weaker than this.

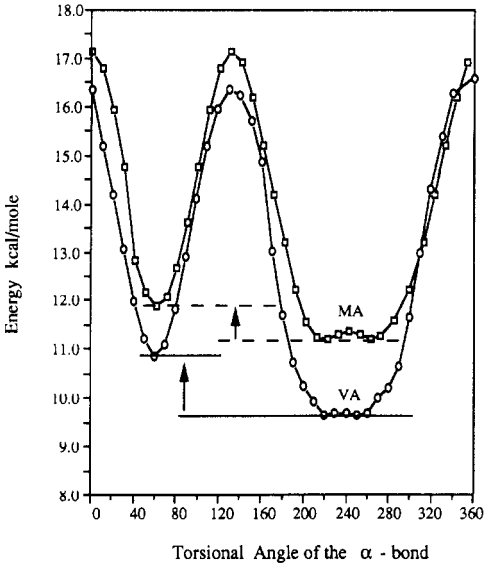

Figure 9. Comparison of energy of rotation of MA-type ester group with that for a VA-type group (at the 4-position on the TTTT heptane). Rotational site energy differences are indicated and are larger for VA than for MA. This leads to strength suppression in VA compared to MA.

The calculated correlation function for the 20 mol % VA/E copolymer has no precise comparison with experiment. The β process is so poorly resolved experimentally from the α glass transition region and the γ lower temperature region that it could only be concluded that the process is somewhat weaker than the γ process.[4] The correlation function for the latter is shown as a dashed line in Figure 8 and it may be seen that the calculations are in accord with this semiquantitative conclusion.

Comparison of Subglass Processes in MA and VA Polymers. The major difference in strength for the subglass processes between MA and VA systems has been emphasized. As already indicated, the strength is largely responsive to the site energy differences for the side-group rotation; see Figure 9. The energy difference is significantly larger for VA side-group rotation and this results in suppression of the strength through the $p(1)p(2)$ and $p(1)p(3)$ terms in eq 30. The difference between the systems, which arises from the different structural direction of attachment of the ester group, is well accounted for by the conformational energy calculations. It is interesting to make some qualitative observations. The VA situation, because the ester carbonyl group is farther

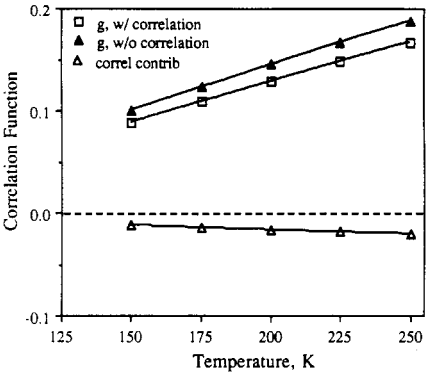

Figure 10. Effect of dipole–dipole correlation on subglass relaxation strength in MA homopolymer. Open triangles are the contribution of $\sum_i\sum_{j\neq i}\langle\mu_i\cdot\mu_j\rangle - \sum_i\sum_{j\neq i}\langle\mu_i\rangle\cdot\langle\mu_j\rangle$ terms in eq 30. Filled triangles are results of eq 30 deleting these terms and open squares are from eq 30 including them.

from the main chain, is inherently less sterically hindered in its lower energy positions (−90° and −150° sites, Figure 9) and has a lower conformational energy than the MA system. On rotation to the 60° site, a fairly serious steric hindrance between the carbonyl and the main chain is generated. In MA, all the side-group positions are more hindered than in VA and thus are less sensitive to rotation.

Site Population versus Dipole–Dipole Correlation in Subglass Strength. For an overall $\alpha + \beta$ process, dipole–dipole correlation only, as expressed, for example, by eq 13, determines the correlation function. However, as seen in eq 30, for subglass processes both site population, $p(r)p(s)$ terms, and dipole–dipole correlation, $\langle\mu_i\cdot\mu_j\rangle - \langle\mu_i\rangle\cdot\langle\mu_j\rangle$, terms contribute. At low temperature, as dipoles settle into the lowest energy site, the population terms approach zero and $\langle\mu_i\cdot\mu_j\rangle \rightarrow \langle\mu_i\rangle\cdot\langle\mu_j\rangle$. Thus the strength goes to zero. It was found computationally for the chain ensembles studied that the population terms dominated over the dipole–dipole correlation terms. MA homopolymer showed the largest dipole–dipole correlation effect in the subglass region. Results for this case are shown in Figure 10 where the effect of the dipole–dipole correlations are seen to be noticeable but relatively minor.

Conclusion. It appears that the concept of side-group reorientation on a dynamically quiescent main chain accounts well for the subglass strength behavior of the two homopolymers, and with some reasonable speculation about the effect of main-chain subglass motion in PE segments the concept of side group reorientation appears to be compatible with the copolymer strengths as well.

Acknowledgment. We are grateful for the following sources of support for our research. The work was supported by the U.S. Army Research Office and by the National Science Foundation, Division of Materials Research, Polymers Program. G. D. Smith was holder of a National Science Foundation Graduate Fellowship and a University of Utah Research Support Committee Fellowship. The computer calculations were carried out under the IBM Corp. RSP program at the Los Angeles Scientific Center and at the University of Utah Supercomputing Institute.

References and Notes

(1) McCrum, N. G.; Read, B. E.; Williams, G. *Anelastic and Dielectric Effects in Polymeric Solids*; Wiley-Interscience: New York, 1967.
(2) Boyd, R. H. *Polymer* **1985**, *26*, 1123.
(3) Buerger, D. E.; Boyd, R. H. *Macromolecules* **1989**, *22*, 2694.
(4) Buerger, D. E.; Boyd, R. H. *Macromolecules* **1989**, *22*, 2699.

(5) Froehlich, H. *Theory of Dielectrics*, 2nd ed.; Oxford University Press: London, 1958.
(6) Smith, G. D.; Boyd, R. H. *Macromolecules*, preceding paper in this issue.
(7) Sundararajan, P. R. *Macromolecules* **1978**, *11*, 256.
(8) Yoon, D. Y.; Suter, U. W.; Sundararajan, P. R.; Fory, P. J. *Macromolecules* **1975**, *8*, 784. Side-group states were included in a later version for oligomers, but no polymer calculations were reported; Yarim-Agaev, Y.; Plavsic, M.; Flory, P. J. *Polym. Prepr.* **1983**, *24* (1), 233.
(9) Tarazona, M. P.; Saiz, E. *Macromolecules* **1983**, *16*, 1128.
(10) Mark, J. E. *J. Chem. Phys.* **1972**, *57*, 2541.
(11) Smith, G. D. Ph.D. Dissertation, University of Utah, 1990.
(12) Salyer, I. O.; Kenyon, A. S. *J. Polym. Sci., Part A-1* **1971**, *9*, 3083.
(13) Schaeffer, J. A. *J. Phys. Chem.* **1966**, *70*, 1975.
(14) Wu, T. K. *J. Polym. Sci., Part A-2* **1970**, *8*, 167.
(15) Wu, T. K.; Ovenall, D. W.; Reddy, G. S. *J. Polym. Sci., Polym. Phys. Ed.* **1974**, *12*, 901.
(16) Bovey, F. A.; Anderson, E. W.; Douglass, D. C.; Manson, J. A. *J. Chem. Phys.* **1963**, *39*, 1199.
(17) Fujii, K. *Macromol. Rev.* **1971**, *5*, 431.
(18) Wu, T. K.; Ovenall, D. W. *Macromolecules* **1974**, *7*, 776.
(19) Matsuzaki, K.; Kanai, T.; Kawamura, T.; Matsumoto, S.; Uryu, T. *J. Polym. Sci., Polym. Chem. Ed.* **1973**, *11*, 961.
(20) Ham, G. R. *Copolymerization*; Wiley-Interscience: New York, 1964.
(21) Raetzsch, M.; Lange, H. *Plast. Kautsch.* **1979**, *26*, 6.
(22) Flory, P. J. *Statistical Mechanics of Chain Molecules*; Wiley-Interscience: New York, 1969.
(23) Flory, P. J.; Mark, J. E.; Abe, A. *J. Am. Chem. Soc.* **1966**, *88*, 639.
(24) Reference 22, p 89.
(25) Reference 22, pp 73–74, eqs 41 and 42.
(26) Reference 5, p 45, eq 7.32.
(27) Hoffman, J. D. *J. Chem. Phys.* **1952**, *20*, 541.
(28) Hoffman, J. D.; Pfeiffer, H. G. *J. Chem. Phys.* **1954**, *22*, 132.
(29) Hoffman, J. D. *J. Chem. Phys.* **1955**, *23*, 1331.
(30) Karunakaran, K.; Santappa, M. *J. Polym. Sci., Part A-2* **1968**, *6*, 713.
(31) Matsuda, H.; Yamano, K.; Inagaki, H. *J. Polym. Sci., Part A-2* **1969**, *7*, 609.
(32) Matsumoto, M.; Ohyanagi, Y. *J. Polym. Sci.* **1961**, *50*, S1.
(33) Boyd, R. H. *Polymer* **1985**, *26*, 323.
(34) Tarazona, M. P.; Saiz, E. *Macromolecules* **1983**, *16*, 1128.
(35) LeFevre, C. G.; LeFevre, R. J. W.; Parkins, G. M. *J. Chem. Soc.* **1960**, 1814.
(36) Takeda, M.; Imamura, Y.; Okamura, S.; Higashimura, T. *J. Chem. Phys.* **1960**, *33*, 631.